Theoretical modeling study of kaolinite by Combining it with TiO_2, ZrO_2, and Al_2O_3

BOUBAKER.M.HOSOUNA*, SALEH.N.AHDIRI
Chemistry Department, Faculty of Sciences, Sebah University, Libya
Corresponding email: bou.hosouna@sebhau.edu.ly*

Submission data: 16/7/2024 Electronic publishing data: 11/8/2024

Abstract: The study found that by adding a group of oxides to modify the properties of the main ingredient, Kaolinite, in ceramics, the addition of aluminum oxide resulted in better results than titanium oxide and zirconium. The physical properties of Kaolinite were also altered, resulting in a change in internal energy (from -1743.441 to -2453.9072 Hartree), the stability increased compared to the case of Kaolinite alone. Additionally, the absorption of the UV-vis is increased from 481.59 nm to 2752 nm. When attempting to add aluminum oxide to Kaolinite, we found that the best ratio was 1:1. Increasing the ratio to 1:2, 1:3, and 1:4 resulted in a significant decrease in internal energy, absorption, and polar determination.

Key words: Kaolinite, Molecular modeling, TiO_2, ZrO_2, and Al_2O_3.

Introduction:

Kaolinite, also known as kaolin, is an earth mineral with the chemical formula $Al_2Si_2O_5(OH)_4$. It is a layered silicate mineral consisting of one octahedral sheet of alumina (AlO6) and one tetrahedral sheet of silica (SiO_4) linked by oxygen atoms. [3]

Kaolinite is a white, delicate, gritty mineral that is a dioctahedral phyllosilicate clay. It is produced through the chemical weathering of aluminum silicate minerals such as feldspar. It has a low therapist expand limit and a low cation-trade limit (1–15 meq/100 g).[4]

Rocks rich in kaolinite and halloysite are known as kaolin or china clay. Kaolin is often coloured pink, orange or red by iron oxide, giving it a distinctive rust tint. The white, yellow or light orange shades of kaolinite are caused by lower levels of iron oxide. Occasionally, alternating lighter and darker layers are found, as at Provision Gully State Park in Georgia, US.[6-7]

Kaolinite is a natural substance that is widely used in various industries and applications. Commercial grade kaolinite is produced and transported in the form of powder, lumps, semi-dried noodles, or slurry. The global production of kaolinite in 2021 was estimated to be 45 million tonnes.[8]

However, in pottery applications, a similar recipe is usually written for oxides, which results in the formation of $Al_2O_3 \cdot 2SiO_2 \cdot 2H_2O$.[9] Although metakaolin has distinct properties, high-energy milling of kaolinite produces a mechanochemically amorphized phase that closely resembles metakaolin. [10] The high-energy milling process is inefficient and consumes a significant amount of energy.[11]

Anti-wear and anti-corrosion applications in harsh environments require hard ceramic coatings [12-16]. Analysts have focused on enhancing the mechanical properties of coatings by incorporating ceramic phases such as TiO2 [17-25] and ZrO2 [26-29]. The main aim of this examination is to establish the relationship between the physical properties and microstructure to enhance the mechanical properties of these composites. The combination of the Hall-Petch effect with nanoparticles [30-34] was observed and interpreted as the cause of the improvement in the stiffness and toughness of alumina matrix nanocomposites.

There have been few investigations on tribological earthenware grid composites containing ceramic or metallic nanoparticles. However, alumina is the most commonly used material as a grid [35-37]. Alumina ceramic is known for its exceptional hardness and strength, although it is generally less sturdy compared to zirconia. On the other hand, zirconia is highly durable and strong, but not particularly hard. The addition of zirconia strong arrangements can enhance the strength and durability of alumina, mainly due to the tetragonal monoclinic change [38-41].

Computational method

After years of developing increasingly precise and computationally expensive semi-empirical models, John realised that improvements to the algorithms could make non-experimental (then called 'ab initio') calculations fast enough to apply to large problems [42]. This type of theory remained his focus for the last thirty years of his work. His paper on the STO-3G basis set remains one of his most cited [43].

After developing a new algorithm with his understudy Warren Hehier, which significantly improved the speed of Haretre Voc accounts, the subsequent program Gaussian 70 [44] was provided through QCPE. Previous projects carried out by other researchers, such as Polyatom, have been presented to numerous academic research groups and their applications. However, due to its speed and convenience, Gaussian 70 has become the primary ab initio program used by many researchers today. The G09 version used in this study was developed based on Gaussian 70.

During the 1970s, John and his team worked on more advanced ab initio strategies, such as larger basis sets (6-31G, 6-31G* [45], etc.) and incorporating electron correlation beyond Hartree-Fock. They also compared several rival methods, including Configuration

Interaction, Perturbation Theory, and Coupled Cluster [46].

This study utilized programs that depend on quantum mechanical conditions and their numerical approximations. The following software was utilized.

HyperChem Professional 08

This PC program improves synthetic mixtures in mathematical space, consolidates compounds, performs rotational energy computations, and examinations bond vibrations.

Gaussian 09

The electronic design bundle has the capacity to foresee different properties of particles, atoms, and intelligent frameworks. Utilizing density functional theory, semi-empirical, molecular mechanics, and hybrid approaches, it is able to draw compounds, calculate bond lengths and angles, and determine bonding energies for those compounds.[47]

Software methods

Computer modeling indicates that the net atomic strength on each atom is close to zero on the surface, resulting in possible energy. Geometry optimization is the process of adjusting the lengths of links and angles of compound atoms to achieve the best engineering shape.

DFT is a regularly involved strategy for working out electronic thickness in different mixtures. It is especially valuable in PC science for treating enormous particles. The DFT strategy is a quantum science technique that depends on the Schrödinger condition. [48]

B3LYP is a technique that is typically employed in the construction of molecular frameworks due to its high degree of precision in the determination of the final calculation, the initial modelling computation, the final energy, and the bond lengths. It is also necessary to consider the lengths of internal bonds and angles. [49]

Problem statement

The previous studies have identified a problem that needs to be addressed: how to enhance the physical qualities and properties of Kaolinite, a main component of ceramics. To achieve this, titanium, zirconia, and aluminum oxides were used as they are known to improve ceramic specifications.

Results and discussion

This study examines the overlap and interaction of titanium, zirconium, and aluminum oxides with kaolinite. The results of the comparison between them are as follows:

For single kaolinite, the results showed internal energy, polar moment, and ultraviolet absorbance of **$Al_2(OH)_4Si_2O_5$.**

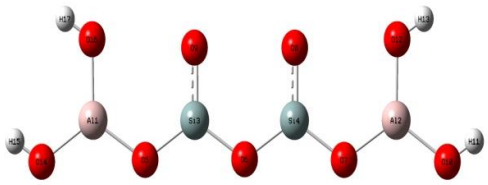

Figure 1 Structural formula of a kaolinite compound

E(TD-HF/TD-DFT) = **-1743.441 Hartree**

Dipole Moment = **0.77163176 Debye**

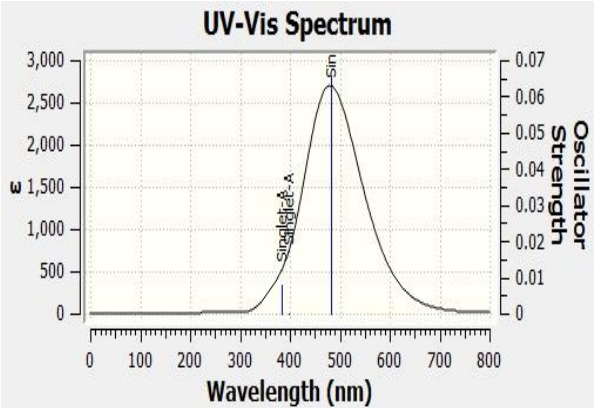

Figure 2 UV spectrum of a kaolinite composite

Uv-vis Absorbance = **481.59 nm**

When titanium oxide was added to kaolinite, the resulting compound was, **$Al_2(OH)_4Si_2O_5$ + TiO_2**

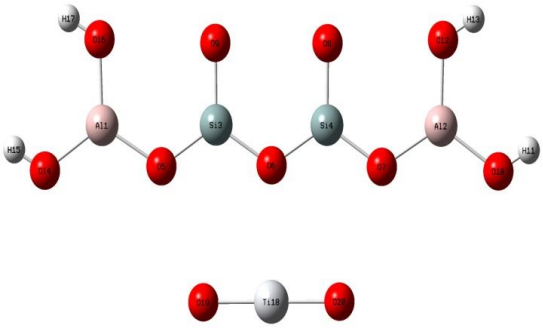

Figure 3 Structural formula for a kaolinite compound with titanium oxide

E(TD-HF/TD-DFT) = **-1952.2426 Hartree**

Dipole Moment = **0.35668813 Debye**

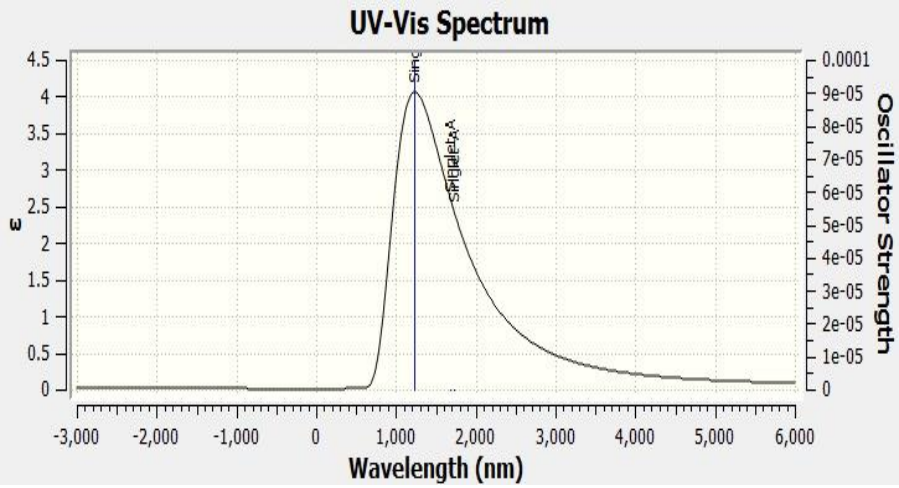

Figure 4 shows the UV spectrum of a composite of kaolinite with titanium oxide

Uv-vis Absorbance =**1726.42 nm**
When zirconium oxide is added to kaolinite, the resulting chemical reaction is **$Al_2(OH)_4Si_2O_5 + ZrO_2$**.

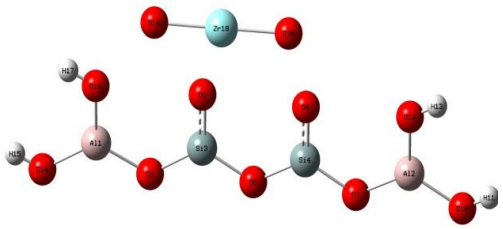

Figure 5 Structural formula for a kaolinite compound with zirconium oxide

E(TD-HF/TD-DFT) = -1941.0145 Hartree
Dipole Moment = 1.8713692 Debye

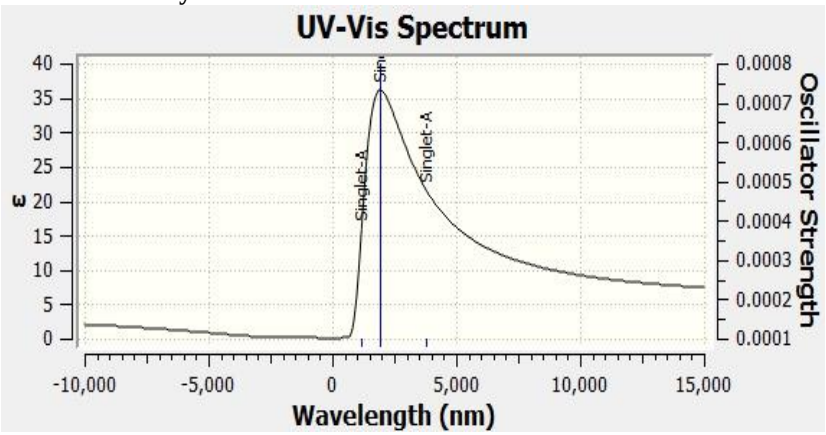

Figure 6 shows the UV spectrum of a composite of kaolinite with zirconium oxide

Uv-vis Absorbance = **1923.45 nm**
Finally, when aluminium oxide is added to kaolinite, the resulting chemical reaction produces, **$Al_2(OH)_4Si_2O_5 + Al_2O_3$**.

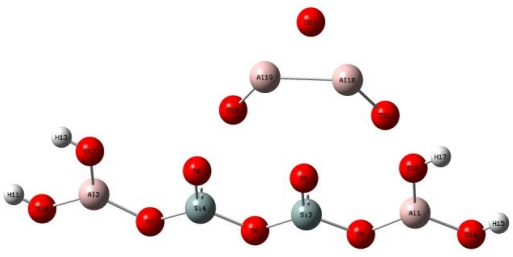

Figure 7 The structural formula for a kaolinite compound with aluminium oxide

E(TD-HF/TD-DFT) = -2453.9072 Hartree
Dipole Moment = 7.1540711 Debye

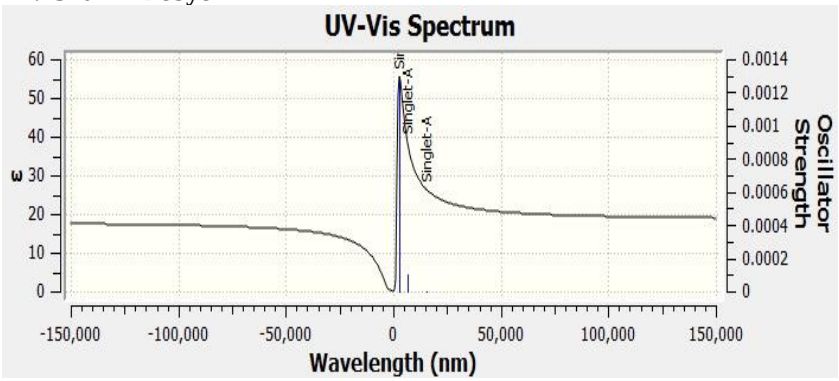

Figure 8 shows the UV spectrum of a kaolinite composite with aluminium oxide

Uv-vis Absorbance = **2752.73 nm**

Table 1 displays the compounds' internal energies, polar moments, and ultraviolet absorption. The table illustrates the relationship between these properties.

Chemical compound	Total internal energy, hartree	Uv-vis Spectrum, nm
$Al_2(OH)_4Si_2O_5$	-1743.441	481.59
$Al_2(OH)_4Si_2O_5 + TiO_2$	-1952.2426	1726.42
$Al_2(OH)_4Si_2O_5 + ZrO_2$	-1941.0145	1923.45
$Al_2(OH)_4Si_2O_5 + Al_2O_3$	-2453.9072	2752.73

Table 1 displays the results of the calculations, highlighting the difference between them and providing a comparison. The interaction with aluminum oxide outperformed that with kaolinite, as demonstrated in Figures 9 and 10, which show the internal energy and ultraviolet absorbance, respectively.

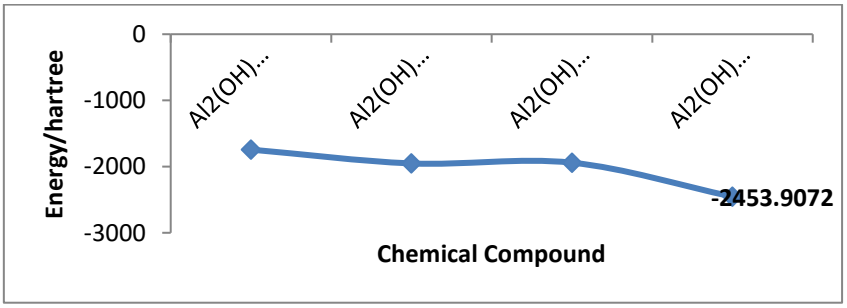

Figure 9 Internal energy curve for oxide complexes with kaolinite

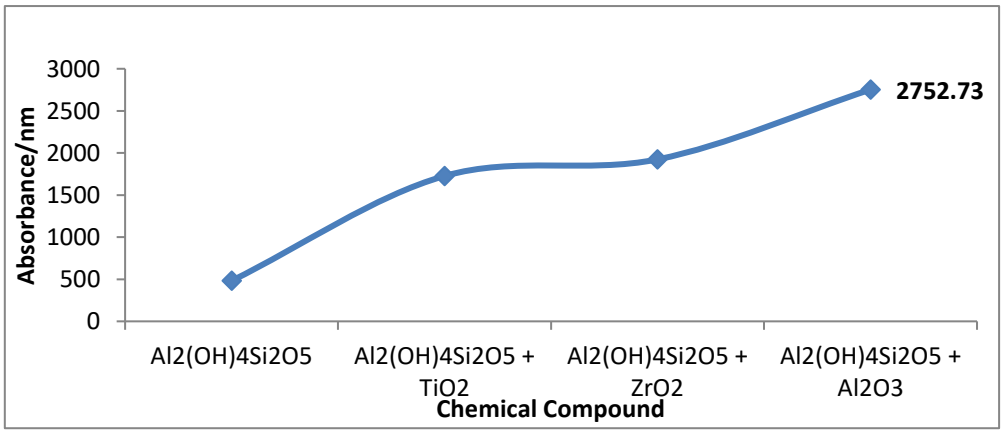

Figure 10 Ultraviolet absorbance values curve for oxide composites containing kaolinite

The results presented in Table 1 and Figures 9 and 10 indicate that the interaction of kaolinite with aluminum oxide produced the best stable energy and best absorption.

The effects of adding a different ratio of aluminium oxide (1:2) to kaolinite. Our aim was to determine its tolerance when mixed with more than one mole of aluminium oxide, **$Al_2(OH)_4Si_2O_5$ + 2 Al_2O_3**.

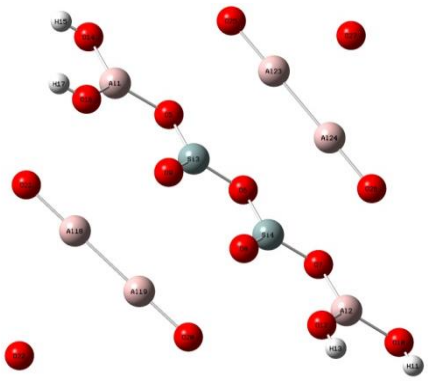

Figure 11 The structural formula for a kaolinite compound with 2 moles of aluminium oxide

E(TD-HF/TD-DFT) = - 3163.952853 Hartree

Dipole Moment = 2.843594 Debye

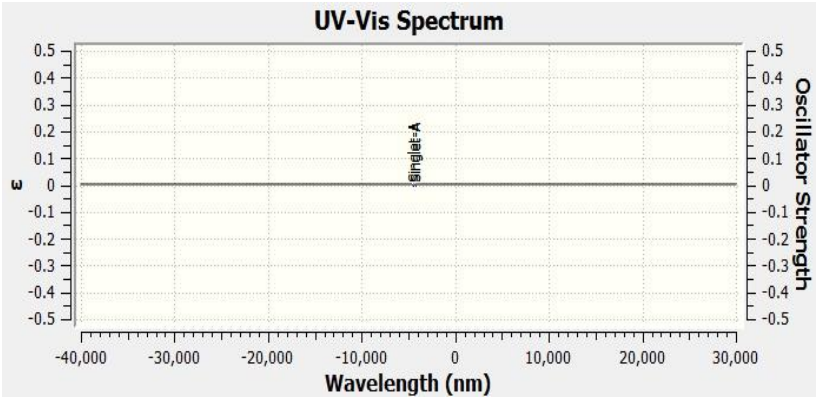

Form 12 shows the UV spectrum of a kaolinite composite with 2 moles of aluminium oxide

Uv-vis Absorbance = **4261.05 nm**

The objective of this investigation was to ascertain the effects of introducing a distinct ratio of aluminium oxide (1:3) to kaolinite. The objective was to ascertain the capacity to withstand the mixing of more than one mole of aluminium oxide, specifically **$Al_2(OH)_4Si_2O_5$ + 3 Al_2O_3**.

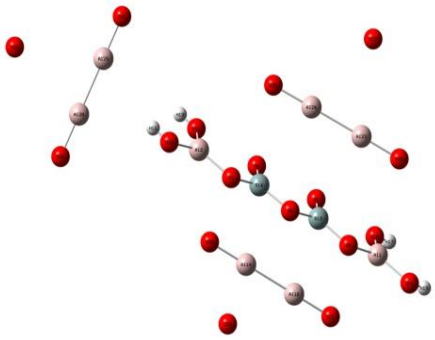

Figure 13 The structural formula for a kaolinite compound with 3 moles of aluminium oxide

E(TD-HF/TD-DFT) = - 3874.15 Hartree

Dipole Moment = 4.2088106 Debye

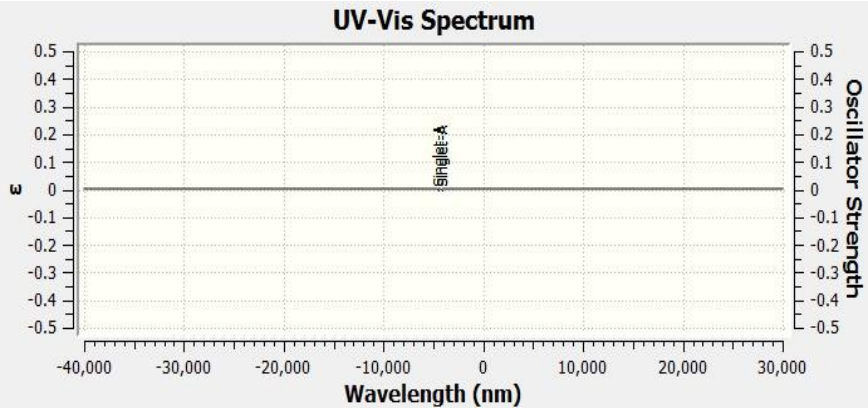

Figure 14 shows the UV spectrum of a kaolinite composite with 3 moles of aluminium oxide

Uv-vis Absorbance = 4173.94nm

The objective of this investigation was to ascertain the effect of introducing a distinct ratio of aluminium oxide (1:4) to kaolinite, with the aim of determining its capacity to interact with a quantity of aluminium oxide in excess of one mole, **$Al_2(OH)_4Si_2O_5$ + 4 Al_2O_3**.

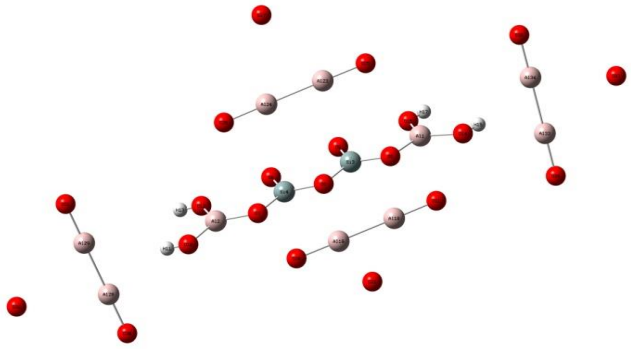

Figure 15 The structural formula for a kaolinite compound with 4 moles of aluminium oxide

E(TD-HF/TD-DFT) = - 4584.359Hartree
Dipole Moment = 3.423973 Debye

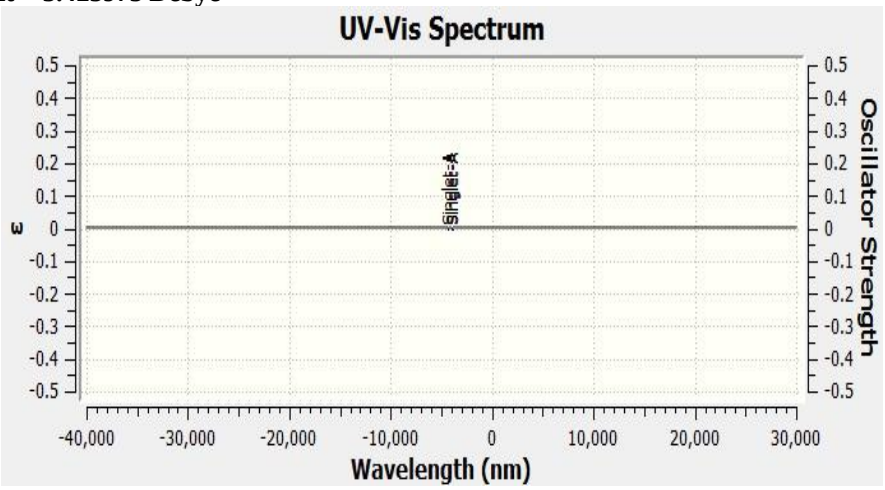

Figure 16 shows the UV spectrum of a kaolinite composite with 4 moles of aluminium oxide

Uv-vis Absorbance = 3928.62 nm

The results of adding different proportions of aluminum oxide to kaolinite from 1:1 to 1:2, 1:3, and finally 1:4, respectively, indicate an imbalance in the results. None of the compounds obtained met all the required specifications due to the low polar moment for all the ratios added at 1:2, 1:3, and 1:4. The polar moment is a crucial factor in this industry as it requires good flexibility for expansion, despite the difference in ambient temperatures. We observed an increase in internal energy and absorption of ultraviolet rays, but these values are not as significant as the polar moment. Therefore, we determined a 1:1 ratio as the optimal interaction between aluminum oxide and kaolinite. Table 2 displays the varying results.

Table 2 shows the internal energy values for the percentages of aluminum oxide overlap with kaolinite.

Chemical compound	Total internal energy, hartree	Spectrum, nm Uv-vis
$Al_2(OH)_4Si_2O_5 + Al_2O_3$	- 2453.907	2752.73
$Al_2(OH)_4Si_2O_5 + 2\ Al_2O_3$	- 3163.952	4261.05
$Al_2(OH)_4Si_2O_5 + 3\ Al_2O_3$	- 3874.150	4173.94
$Al_2(OH)_4Si_2O_5 + 4\ Al_2O_3$	- 4584.359	3928.62

Conclusion

This study demonstrated that the internal composition of the ceramic, which is kaolinite, can be improved by the addition of a group of oxides. The study concluded that this approach yielded superior results compared to the use of a single oxide. In particular, the addition of titanium oxide, zirconium oxide, and aluminium oxide to kaolinite resulted in a notable enhancement in the physical characteristics. Furthermore, an alteration in the internal energy was observed, with a change from -1743.441 to -2453.9072 Hartree. The addition of the Al_2O_3 group to kaolinite resulted in a notable enhancement in stability compared to that observed in kaolinite alone. Furthermore, the dipole moment exhibited a notable increase from 0.77163176 to 7.1540711 Debye, thereby conferring upon the composite material considerable flexibility and durability. Furthermore, the composite demonstrated enhanced absorption, with a notable increase from 481.59 to 2752 nm. In attempting to add aluminium oxide to kaolinite, the optimal ratio was determined to be 1:1. An increase in the ratio to 1:2, 1:3 and 1:4 resulted in a notable reduction in internal energy, absorption and polarity determination.

References

1. Anthony JW, Bideaux RA, Bladh KW, et al., eds, (1995).
2. "kaolinite". Lexico UK English Dictionary. Oxford University Press. (2021).
3. Deer WA, Howie RA, Zussman J. An Introduction to the Rock-forming Minerals (2nd ed.), (1992).
4. Murray, H.H. Traditional and new applications for kaolin, smectite, and palygorskite: A general overview. Appl. Clay Sci, (2000).
5. Pohl WL, Economic geology: principles and practice: metals, minerals, coal and hydrocarbons – introduction to formation and sustainable exploitation of mineral deposits. Chichester, West Sussex: Wiley-Blackwell, (2011).
6. Detellier, C. Functional kaolinite. Chem. Rec, (2018).
7. Miranda-Trevino, J.C.; Coles, C.A. Kaolinite properties, structure and influence of metal retention on pH. Appl. Clay Sci, (2003).
8. 'U.S. Geological Survey, Mineral Commodity Summaries, (2022).
9. Perry DL, Handbook of Inorganic Compounds (2nd ed.). Boca Raton: Taylor & Francis, (2011).
10. Kasa E, Szabados M, Baan K, Konya Z, Kukovecz A, Kutus B, Palinko I, Sipos P, (2021).
11. Baláž, Peter, "High-Energy Milling". Mechanochemistry in Nanoscience and Minerals Engineering, (2008).
12. Wang m, leon l s. effects of the powder manufacturing method on microstructure and wear performance of plasma sprayed alumina–titania coatings [j]. surface and coatings technology, 2007, 202(1): 34−44.
13. Keyvani a. microstructural stability oxidation and hot corrosion resistance of nanostructured al2o3/ysz composite compared to conventional ysz tbc coatings [j]. journal of alloy and composite, 2015, 623: 229−237.
14. Zhang j, kobayashi a. corrosion resistance of the al2o3−zro2 thermal barrier coatings on stainless steel substrates [j].vacuum, 2008, 83(1): 92−97.
15. Rico a, rodriguez j, otero e, zeng p, rainforth w m. wear behaviour of nanostructured alumina–titania coatings deposited by atmospheric plasma spray [j]. wear, 2009, 267(5−8): 1191−1197.
16. Limarga m a, sujanto w, hon y t. mechanical properties and oxidation resistance of plasma-sprayed multilayered al2o3/zro2 thermal

barrier coatings [j]. surface and coatings technology, 2005, 197(1): 93−102.

17. Lu x, yan d r, yang y, dong y c, he j n, zhang j x. phase evolution of plasma sprayed al2o3−13%tio2 coatings derived from nanocrystalline powders [j]. transactions of nonferrous metals society of china, 2013, 23(10): 2951−2956.
18. Jia s k, zou y, xu j y, wang j, yu l. effect of tio2 content on properties of al2o3 thermal barrier coatings by plasma spraying [j]. transactions of nonferrous metals society of china, 2015, 25(1): 175−183.
19. He long, tan ye-fa, tan hua, zhou chun-hua, gao li. tribological properties of nanostructured al2o3−40%tio2 multiphase ceramic particles reinforced ni-based alloy composite coatings [j]. transactions of nonferrous metals society of china, 2013, 23(9): 2618−2627.
20. Younes r, bradai m a, sadeddine a, mouadji y, bilek a, benabbas a. microstructural and tribological properties of al2o3−13pcttio2 thermal spray coatings deposited by flame spraying [j]. metallurgical and materials transactions b, 2015, 46(5): 2394−2403.
21. Gao jia-cheng, zou jian, tan xiao-wei, wang yong. characteristics and properties of surface coated nano-tio2 [j]. transactions of nonferrous metals society of china, 2006, 16(6): 1252−1258.
22. Estili m, kawasaki a, sakamoto h, mekuchi y, kuno m, tsukada t. the homogeneous dispersion of surfactant less, slightly disordered, crystalline, multiwalled carbon nanotubes in α-alumina ceramics for structural reinforcement [j]. acta materialia, 2008, 56(15): 4070−4079.
23. Yao lei, liu jian-hua, yu mei, li song-mei, wu hao. formation and capacitance properties of ti−al composite oxide film on aluminum [j]. transactions of nonferrous metals society of china, 2010, 20(5): 825−830.
24. Bahramian a, raeissi k, hakimizad a. an investigation of the characteristics of al2o3/tio2 peo nanocomposite coating [j]. applied surface science, 2015, 351(1): 13−26.
25. Perumal g, geetha m, asokamani r, alagumurthi n. wear studies on plasma sprayed al2o3−40% 8ysz composite ceramic coating on ti−6al−4v alloy used for biomedical applications [j]. wear, 2014, 311(1−2): 101−113.
26. Su hai-jun, zhang jun, liu lin, fu heng-zhi. effects of laser processing parameters on solidification microstructures of ternary al2o3/yag/zro2 eutectic in situ composite and its thermal property [j]. transactions of nonferrous metals society of china, 2009, 19(6): 1533−1538.
27. Srinivasan p b, liang j, blawert c, dietzel w. dry sliding wear behaviour of magnesium oxide and zirconium oxide plasma electrolytic oxidation coated magnesium alloy [j]. applied surface science, 2010, 256(10): 3265−3273.
28. Khalil a, kim s w. mechanical wet-milling and subsequent consolidation of ultra-fine al2o3−(zro2+3%y2o3) bioceramics by using high-frequency induction heat sintering [j]. transactions of nonferrous metals society of china, 2007, 17(1): 21−26.
29. Liang b, zhang g, liao h l, coddet c, ding c x. friction and wear behavior of zro2−al2o3 composite coatings deposited by air plasma spraying: correlation with physical and mechanical properties [j]. surface and coatings technology, 2009, 203(20−21): 3235−3242.
30. Oh s t, sekino t, nihara k. fabrication and mechanical properties of 5 vol, percent copper dispersed alumina nanocomposite [j]. journal of the european ceramic society, 1998, 18(1): 31−37.
31. Mishra r.s, mukherejee a k. processing of high hardness- high toughness alumina matrix nanocomposites [j]. materials science and engineering a, 2001, 301(1): 97−101.
32. An j w, you d h, lim d s. tribological properties of hot-pressed alumina−cnt composites [j]. wear, 2003, 255(1−6): 677−681.
33. Datcheva m, cherneva s, stoycheva m, iankova r, stoychev d. determination of anodized aluminum material characteristics by means of nanoindentation measurements [j]. materials sciences and applications, 2011, 2: 1452−1464.
34. Cherneva s, iankova r, radic n, grbic b, stoycheva d. nanoindentation investigation of mechanical properties of zro2, zro2−y2o3, al2o3 and tio2 thin films deposited on stainless steel oc404 substrate by spray pyrolysis [j]. materials science and engineering b, 2014, 183: 12−16.
35. Tazegul o, muhaffel f, meydanoglu o, baydogan m, kayali e s, cimenoglu h. wear and corrosion characteristics of novel alumina coatings produced by micro arc oxidation on az91d magnesium alloy [j]. surface and coatings technology, 2014, 258: 168−173.
36. Kim s h, hannula s p, lee s w. effects of the sliding conditions on the tribological behavior of atmospheric plasma sprayed al2o3−15wt% zro2−caf2 composite coating [j]. surface and coatings technology, 2012, 210: 127−134.
37. Zhou yue-bo, chen hong-yu, zhang hai-jun, wang yong-dong. oxidation of al2o3-dispersion chromizing coating by pack-cementation at 800 °c [j]. transactions of nonferrous metals society of china, 2008, 18(3): 598−602.
38. Zhao xiao-qin, an yu-long, chen jian-min, zhou hui-di, yin bin. properties of al2o3−40wt%zro2 composite coatings from ultra-fine feedstocks

by atmospheric plasma spraying [j]. wear, 2008, 265(11−12): 1642−1648.

39. Volceanov e, volceanov a, stoleriu ş. assessment on mechanical properties controlling of alumina ceramics for harsh service conditions [j]. journal of european ceramic society, 2007, 27: 759−762.
40. Hori s, kurita r, yoshimura m, somiya s. suppressed grain growth in final stage sintering of al2o3 with dispersed zro2 particles [j]. journal of materials science letters, 1985, 4(9): 1067−1070.
41. Messing l g, kumangi m. low-temperature sintering of seeded sol-gel derived, zro2-toughened al2o3 composites [j]. journal of the american ceramic society, 1989, 72(1): 40−44.
42. M. D. Newton, W. A. Lathan, W. J. Hehre, and J. A. Pople, "Self-Consistent Molecular Orbital Methods. III. Comparison of Gaussian Expansion and PDDO Methods Using Minimal STO Basis Sets," *J. Chem. Phys*. **51** (1969) 3927.
43. W. J. Hehre, R. F. Stewart, and J. A. Pople, "Self-Consistent Molecular Orbital Methods I. Use of Gaussian Expansions of Slater Type Atomic Orbitals," *J. Chem. Phys*. **51** (1969) 2657.
44. W. J. Hehre, W. A. Lathan, R. Ditchfield, M. D. Newton, and J. A. Pople, *Gaussian 70* (Quantum Chemistry Program Exchange, Program No. 237, 1970).
45. P. C. Haharan and J. A. Pople, "The Influence of Polarization Functions on Molecular Orbital Hydrogenation Energies," *Theor. Chim. Acta* **28** (1973) 213.
46. Important papers include: J. S. Binkley and J. A. Pople, "Møller-Plesset Theory for Atomic Ground State Energies," *Int. J. Quant. Chem*. **9** (1975) 229; J. A. Pople, J. S. Binkley, and R. Seeger, "Theoretical Models Incorporating Electron Correlation," *Int. J. Quant. Chem*. **10** (1976) 1; J. A. Pople, R. Seeger, and R. Krishnan [K. Raghavachari], "Variational Configuration Interaction Methods and Comparison with Perturbation Theory," *Int. J. Quant. Chem*. **S11** (1977) 149.
47. Tsuji M, Homology Modeling Professional for HyperChem, revision G1, Institute of Molecular Function, Saitama, Japan, (2015).
48. Tsuji M, Docking Study with HyperChem, revision G1, Institute of Molecular Function, Saitama, Japan, (2015).
49. HyperChem Professional, version 8.0.10, Hypercube, Inc., Gainesville, Florida, USA.

الملخص : توصلت الدراسة إلى أنه بإضافة مجموعة من الأكاسيد لتعديل خواص المكون الرئيسي للكاولينيت في السيراميك فإن إضافة أكسيد الألومنيوم أدى إلى نتائج أفضل من أكسيد التيتانيوم والزركونيوم. كما تغيرت الخواص الفيزيائية للكاولينيت مما أدى إلى تغير الطاقة الداخلية من 1743.441- إلى 2453.9072 - هارتري، وزاد الثبات مقارنة بحالة الكاولينيت وحده. بالإضافة إلى ذلك، تم زيادة امتصاص الأشعة الفوق بنفسجية من 481.59 إلى 2752 نانومتر. عند محاولة إضافة أكسيد الألومنيوم إلى الكاولينيت، وجدنا أن النسبة الأفضل كانت 1:1 أدت زيادة النسبة إلى 1:2 و1:3 و1:4 إلى انخفاض كبير في الطاقة الداخلية والامتصاص.

مفتاح الكلمات: الكاولينيت، النمذجة الجزيئية، أكسيد التيتانيوم، أكسيد الزركونيوم و أكسيد الألومنيوم.